

Ultrasound Assisted Green Synthesis and Characterization of Graphene Oxide

A. Farazas¹, A. Mavropoulos^{1,*}, D. Christofilos², I. Tsiaoussis³ and D. Tsipas¹

¹Department of Mechanical Engineering, Faculty of Engineering, Aristotle University of Thessaloniki, Thessaloniki, Greece.

²Department of Chemical Engineering, Faculty of Engineering, Aristotle University of Thessaloniki, Thessaloniki, Greece.

³School of Physics, Faculty of Sciences, Aristotle University of Thessaloniki, Thessaloniki, Greece.

(*) Corresponding author: azarias@auth.gr

(Received: 31 May 2017 and Accepted: 04 July 2017)

Abstract

Graphene oxide (GO) was prepared by an improved green chemical method using graphite flakes, $KMnO_4$, a mixture of H_2SO_4/H_3PO_4 , H_2O_2 and HCl . In several stages, ultrasound was used to separate the oxidized layers of GO. The use of ultrasound optimizes the effect of the reacting agents, decreasing the required amounts of used chemicals. This method produces graphene oxide highly oxidized with greater interlayer spacing over the Hummers' method without producing toxic gases. The final product was characterized by UV-VIS, XRD, optical microscopy, TEM and Raman Spectroscopy and all used techniques verified the desirable outcome. The results showed that this low cost method is fully scalable without producing undesirable environmental effects.

Keywords: Graphene oxide, Green synthesis, Ultrasound.

1. INTRODUCTION

Graphene is an allotrope of elemental carbon with a single layer of sp^2 carbon atoms arranged into a two dimensional honeycomb lattice [1]. It features extraordinary electronic properties as it is a zero gap semiconductor, with high mechanical stiffness [2] and excellent thermal conductivity [3,4], making it ideal for several applications in electronics, batteries [5] and biomedicine [6,7]. Since the first production of single layer graphene, graphene gained great attention by the scientific community and several methods were invented to produce high quality graphene in large scale. Although the first method was mechanical exfoliation of graphite, this technique is not effective for producing large quantities. So, other methods like chemical vapor deposition (CVD), epitaxial growth and chemically derived graphene have been suggested [8]. Methods using chemical means are easily scalable as they allow to

produce large quantities of graphene. The challenge in all methods that use bulk graphite to produce graphene is to overcome the Van der Waals forces that attach the layers of graphene together. The main chemical techniques for graphite exfoliation include the intercalation, the chemical modification and the oxidation-reduction.

The presence of compounds such as carboxyl, carbonyls and alcohols groups on the basal plane of graphene oxide reduces the interlayer forces, increasing the interlayer spacing from 0.335nm to around 0.625nm and allowing layers to separate easier. So, the initial oxidation of graphite and the following reduction to obtain reduced graphene oxide (rGO) is one of the proposed simple chemical methods [9] to produce sequentially GO, rGO and finally graphene. Despite the significant recent research on graphene and graphene oxide, historically, graphene oxide production has

been reported since 1859 when Brodie [10] first announced the synthesis of graphene oxide by adding potassium chlorate into slurry of graphite in fuming nitric acid. Several years later in 1898 Staudenmaier [11] improved Brodie's procedure by using concentrated sulfuric acid combined with fuming nitric acid and adding the chlorate in multiple aliquots over the course of the reaction. The obtained graphene oxide by the Staudenmaier method had better qualitative characteristics than the one produced by Brodie and it was easier to produce as it was done in a single step-reaction. Despite the progress made by the above proposed methods for GO preparation, the proposed procedures by Brodie and Staudenmaier have a significant risk of explosion and so they could not be scaled up. In 1958 Hummers [12] invented a new method of oxidizing graphite by adding KMnO_4 and NaNO_3 in concentrated H_2SO_4 . The Hummers' method was slightly safer than Brodie's and Staudenmaier's and was widely used until today. However, all these methods include the production of highly toxic gases such as NO_2 , N_2O_4 and ClO_2 . With the concern of environmental protection for large scale production, a green and safer GO preparation method was necessary. In 2010, a green synthesis method of graphene oxide was reported by Marcano [9], who produced GO by adding KMnO_4 in a 9:1 mixture of concentrated $\text{H}_2\text{SO}_4/\text{H}_3\text{PO}_4$. The advantages of the Marcano's method were its higher yield and the elimination of toxic gas production during the process compared to the other methods. However, some parameters of the method, for example the influence of the quantity of graphite, the quantity of KMnO_4 , reaction time, and temperature on GO preparation have not been fully optimized. In the present work, graphene oxide was synthesized by an improved green method using KMnO_4 and mixture of concentrated $\text{H}_2\text{SO}_4/\text{H}_3\text{PO}_4$ as oxidizing agents, similar to the method reported by Marcano et al. but with some modifications

and the assistance of ultrasound, as most of the recent methods require energy input from shaking [13], stirring or other way. The obtained GO was characterized by XRD, UV-Vis, optical and electron microscopy as well as Raman spectroscopy.

2. EXPERIMENTAL

2.1. Materials

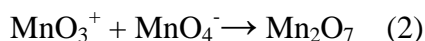
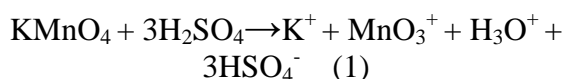
For the synthesis of the graphene oxide natural flake graphite (~325 mesh, $\geq 99.8\%$ purity) was purchased from Alfa Aesar. Concentrated sulfuric acid (95-98%), hydrogen peroxide ($\geq 30\%$) and hydrochloric acid (36-38%) were purchased from Merck, potassium permanganate from Chem-Lab, and phosphoric acid was purchased from Sigma Aldrich. Deionized water was distilled by a laboratory water purification system.

2.2. Sample Preparation

Initially, 3gr of graphite flakes and 9gr of KMnO_4 were added gradually to a 9:1 mixture of concentrated $\text{H}_2\text{SO}_4/\text{H}_3\text{PO}_4$ (180:20 ml) so that not to exceed 55°C . Then the solution was placed in a heated stirrer for 24 hours in 40°C . After the necessary time 1 liter of distilled water and 20ml of H_2O_2 were added. The product was placed in an ultrasound device for 15 minutes and was filtered with a metallic filter of $45\mu\text{m}$ (325mesh). The liquid part was filtered again with polyester fiber and then was washed 3 times with 260ml of HCl keeping every time the solid material. The obtained material was dispersed in water (700ml) with mechanical agitation. Then, the solution was placed in a standard ultrasound device for 15 minutes and was centrifuged initially at 3000rpm for 10 minutes keeping the supernatant and then at 15.000rpm for 10 minutes keeping the bottom product. The second step of centrifugation was repeated until the ph of the solution reached 7. The final material was dispersed in water.

2.3. Chemical Interpretation of the Experimental Procedure

In order to synthesize graphene oxide several materials were used together with the graphite flakes, each with a specific role. Potassium permanganate in the presence of sulfuric and phosphoric acid was used as oxidizing agent. It reacts with sulfuric acid producing diamanganese heptoxide as final product, according to the following reactions (1,2), which causes greater oxidation on graphene flakes[14].



Also, phosphoric acid helps further the penetration of the oxidizing agent between the flakes contributing to better oxidation. Hydrogen peroxide has been used to neutralize the remaining potassium permanganate and the consecutively washes with hydrochloric acid to remove metallic ions from the solution. The application of ultrasound treatment supplies the necessary energy to graphene layers in order to detach each other and thus to facilitate the access of oxidizing agent between the layers. This specific procedure does not produce toxic gases and therefore has the potential for large scale application.

3. RESULTS AND DISCUSSION

3.1. Specific Surface Area Measurement.

The specific surface area of the obtained graphene oxide was measured by BET method. The theoretical value of graphene is $2600\text{m}^2\text{g}^{-1}$ [15], the resulting material was measured to be $557\text{m}^2\text{g}^{-1}$. This could be due to incomplete exfoliation during the ultrasound stages.

3.2. UV-VIS Spectra Analysis

A sample of the final product was analyzed by UV-VIS spectroscopy in order to better understand the nature of the obtained material and the results are shown

in Figure 1. In literature [9], graphene oxide exhibits a main peak at around 230nm and a second peak at lower absorption levels, around 295nm. The peak at 230nm is associated with the $\pi \rightarrow \pi^*$ transitions of $-\text{C}=\text{C}-$ bonds, while that at 295nm with the $n \rightarrow \pi^*$ transitions of the $-\text{C}=\text{O}$ bonds of the carbonyl groups. The results of our samples show a main peak at 231nm and a second smaller peak at 295nm, verifying that the aromatic rings are attached at the surface of the graphene.

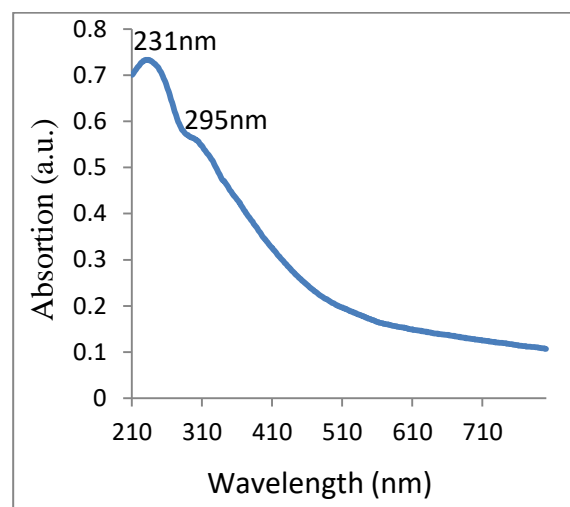


Figure 1. UV-VIS spectra of the graphene oxide sample.

3.3. XRD Analysis

The degree of oxidation of graphene layers was investigated by means of X-ray diffraction. Generally, XRD can detect the interlayer spacing which is directly linked to the degree of oxidation. Greater interlayer distance means less energy needed to detach the layers. In the literature, typical diagrams of graphene oxide for various methods show peaks between 9° and 11° (2θ degree) [9]. The variation of the value is related to the degree of oxidation, which can be explained using the Bragg's law of diffraction, $n\lambda = 2d\sin\theta$. So, smaller θ angles correspond to greater interlayer spacing, which in turn corresponds to greater oxidation. In the XRD diagram of our sample in Figure 2, a peak appears at 9.6° , suggesting an interlayer spacing d of

9.2Å. The results show that the degree of oxidation is higher than Hummers 'method as the interlayer spacing in that method is only 8Å [9].

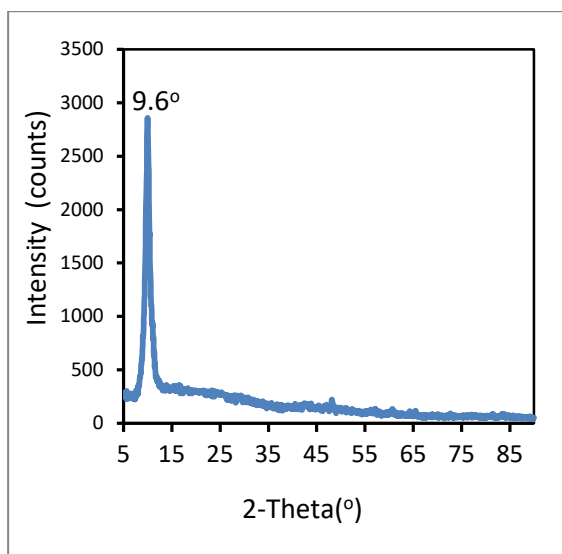


Figure 2. XRD pattern of the graphene oxide sample (0.154059nm Cu Ka 1 as wavelength).

3.4. Optical Microscopy

In the optical microscope, two different samples were examined in order to evaluate the differences in the morphological characteristics of the obtained GO with and without the stages of ultrasound treatment. The first sample was produced as described in the experimental

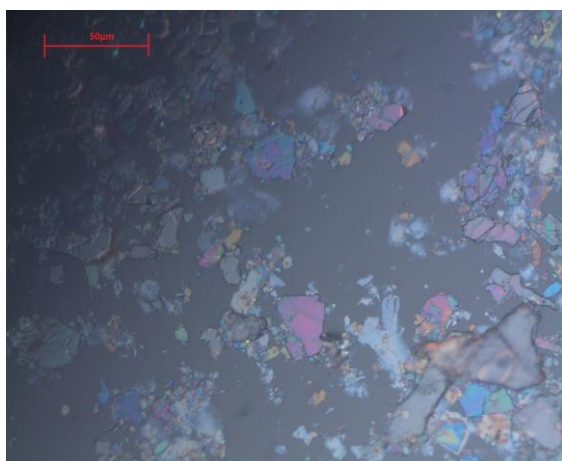


Figure 3. Optical image of a graphene oxide sample prepared without any ultrasound treatment stages.

procedure and the second with the same method but eliminating all the ultrasound stages. In this way we can analyze the effects of ultrasound in the final products

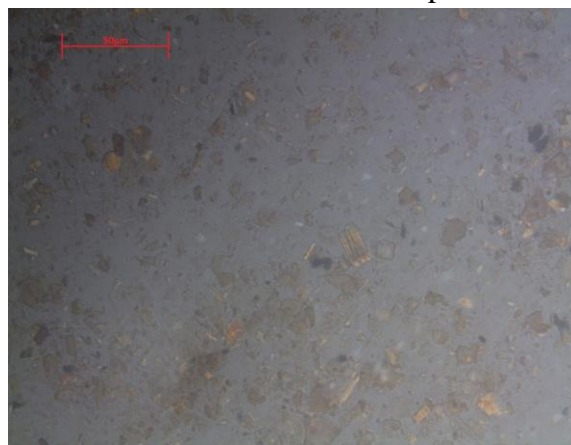


Figure 4. Optical image of a graphene oxide sample prepared including the ultrasound treatment stages.

In Figures 3 and 4 we present the microstructural characteristics of the two samples. The main differences that are immediately observed are the differences in color, size and dispersion of the GO layers. The sample prepared including the ultrasound treatment stages (Figure 4) seems to have uniform light brown coloring compared to the sample without ultrasound treatment (Figure 3), which has more intense colors. The size of the produced GO sheets is smaller in Figure 4, with better dispersion as ultrasound helps the layers to detach each other and disperse uniformly. In Figure 3, the blue color is associated with the presence of $\text{H}_2\text{SO}_4/\text{HSO}_4^-$ into the layers and the purple with the presence of $\text{H}_2\text{SO}_4/\text{HSO}_4^-$ mixture and the oxidizing agent [16]. The remaining colors are the result of the combination of the above colors with the brown-yellowish color of the GO. The number of the layers that are still attached to each other also affects the brightness.

3.5. TEM Measurements

To understand the morphological features of GO, prepared via an improved green chemical method, transmission electron microscopy (TEM) was used to investigate

the final product and LM images have been taken as well as SAED patterns. The existence of multi-layered graphene architecture in GO was also confirmed by TEM, XRD and Raman analysis. Although in some places single-layer graphite sheets are visible, indicated by white arrows.

Furthermore, selected area electron diffraction (SAED) patterns reveal the existence of nanocrystalline areas of GO. The two diffraction rings, with d-spacing of 0.213nm and 0.123nm correspond to grapheme crystal planes (0-110) and (1-210) respectively [17].

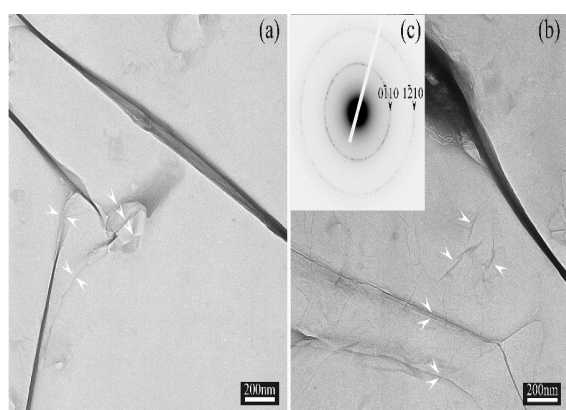


Figure 5. Low Magnification figures have been taken in different places of the specimen showed the presence of wrinkles, ripples and scrolls a) , b) occurrence of few-layered graphene sheets showed by double opposite white arrows, single-layer graphite sheets by one arrow, c) SAED pattern reveal the existence of nanocrystalline areas of GO.

3.6. Raman Spectroscopy

Raman spectroscopy is a powerful tool for the study and characterization of graphitic materials [18,19]. The Raman spectrum of defect-free graphene exhibits a strong peak at $\sim 1580\text{ cm}^{-1}$, the so-called G-band, associated with in-plane C-C vibrations where the hexagons are deformed, and a stronger one at $\sim 2690\text{ cm}^{-1}$, the 2D band. It is the second order mode of the breathing vibration of the hexagons, which is Raman-inactive due to the symmetry. The presence of defects is clearly evident in the Raman spectrum [20] and apart the broadening of all bands, it

activates the D band rendering it visible in the Raman spectrum at around 1350 cm^{-1} (for excitation at $\sim 515\text{ nm}$). Its intensity, relative to that of the G band, is an indicator of the defects concentration. Another defect related peak, D' rises around 1620 cm^{-1} along with other overtones and combinational modes at 2500 to 3200 cm^{-1} .

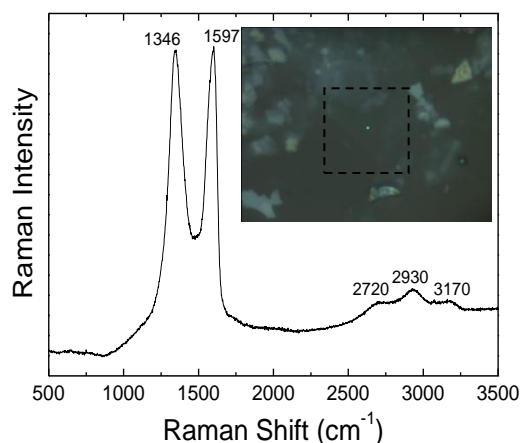


Figure 6. Typical Raman spectrum of the graphene oxide sample. The signal is averaged over an area of $10 \times 10\ \mu\text{m}^2$ (dashed rectangle) where, visually, few GO layers are present (inset).

Raman measurements were conducted with a T64000 (Horiba) spectrometer operating at the single stage mode, equipped with a LN_2 -cooled charge coupled device (CCD). Excitation was provided by a diode-pumped solid state laser (Cobolt), providing a laser beam at 514.5 nm with a laser power of $\sim 100\ \mu\text{W}$ on the sample and focused by a standard 100x objective in a spot with a diameter of $\sim 1\ \mu\text{m}$. Signal was averaged over an area of $10 \times 10\ \mu\text{m}^2$, appropriately scanning the sample under the laser beam in a fast pace. Thus, the light exposure of the sample is very low, avoiding any laser induced effects without reduction in the Raman signal, while the resulting Raman spectrum is more representative of the sample. A typical Raman spectrum of the graphene oxide sample is presented in figure 6. The particular sample was prepared with a

centrifugation stage of 15000 rot/min where a lot of few layers graphene oxide area can be visually identified. However, the main features of the spectrum remain essentially the same at areas with more layers or samples centrifuged at lower centrifugation speeds. The most prominent bands appear at ~ 1346 and ~ 1597 cm^{-1} , related to the D and the closely lying G and D' bands, respectively, with the D and D' bands exhibiting significant intensity. At higher frequencies, a broad feature of small and modulated intensity appears, peaking at 2720, 2930 and 3170 cm^{-1} . It originates from the 2D, D+D', 2D' and possibly other combinational modes. The observed features are compatible with the disorder and defects related to the functionalization of graphene to yield GO. They are in accordance with Raman spectra reported in the literature for GO [21,22]. Moreover, the Raman spectrum appears on a fluorescence background, also typical of GO, which has been previously attributed predominantly to the electron transitions among/between the non-oxidized carbon regions (-C=C-) and the boundary of

oxidized carbon atom regions (C-O, C=O and O=C-OH) for the case of as prepared GO in water [23].

4. CONCLUSIONS

In summary, a simple ultrasound assisted green synthesis method of graphene oxide was presented in the current paper. This method provides significantly better results over the Hummers' method with greater interlayer spacing's, higher degree of oxidation and production of non toxic gases during the preparation procedure. The GO production and quality studied by XRD, UV-VIS and Raman spectroscopy suggest that this method can be used for large scale production since no complex and expensive equipment required.

ACKNOWLEDGEMENT

Authors are thankful to the Center of Interdisciplinary Research and Innovation of the Aristotle University of Thessaloniki (KEΔEK) for the access to the Raman instrumentation.

REFERENCES

1. Slonczewski, J. C., Weiss, Pr., (1958). "Band structure of graphite", *Phys. Rev.*, 109: 272.
2. Yoo, E., Kim, J., Hosono, E., Zhou, H-s., Kudo, T., Honma, I., (2008). "Large reversible Li storage of grapheme nanosheet families for use in rechargeable lithium ion batteries", *Nano Lett.*, 8: 2277-2282.
3. Lee, C., Wei, X., Kysar, J.W., Hone, J., (2008). "Measurement of the elastic properties and intrinsic strength of monolayer graphene", *Science*, 321: 385-388.
4. Ghozatloo, A., Shariaty Niassar, M., Rashidi, A., (2017). "Effect of Functionalization Process on Thermal Conductivity of Graphene Nanofluids", *Int. J. Nanosci. Nanotechnol.*, 13(1): 11-18.
5. Balandin, A. A., Ghosh, S., Bao, W., Calizo, I., Teweldebrhan, D., Miao, F., (2008). "Superior thermal conductivity of single-layer graphene", *Nano Lett.*, 8: 902-907.
6. Berger, C., Song, Z. M., Li, T. B., Li, X. B., Ogbazghi, A. Y., Feng, R., (2004). "Ultrathin epitaxial graphite: 2D electron gas properties and a route toward graphene-based nanoelectronics", *Phys. Chem. B.*, 108: 19912-19916.
7. Sabbaghi-Nadooshan, R., Siasar Karbasaki, M., (2017). "Diagnosis GLY120 Antigen for the Blood and Breast Cancers Using Graphene Nanosheet", *Int. J. Nanosci. Nanotechnol.*, 13(4): 327-333.
8. Berger, C., Song, Z. M., Li, T. B., Li, X. B., Ogbazghi, A. Y., Feng, R., (2004). "Ultrathin epitaxial graphite: 2D electron gas properties and a route toward graphene-based nanoelectronics", *Phys. Chem. B.*, 108: 19912-19916.
9. Marcano, D. C., Kosynkin, D. V., Berlin, J. M., Sinitskii, A., Sun, Z., Slesarev, A., Alemany, L. B., Lu W., and Tour, J. M., (2010). "Improved Synthesis Of Graphene Oxide". *ACS Nano.*, 4(8):4806-4814.
10. Brondie, B. C., (1859). "On the Atomic Weight of Graphite", *Philosophical Transactions of the Royal Society of London*, 149: 249-259.
11. Staudenmaier, L., (1898). "Verfahren zur Darstellung der Graphits", *Ber Dtsch Chem Ges.*, 31: 1481-1487.
12. Hummers, W. S., Offeman. R.E., (1958). "Preparation of Graphitic Oxide", *J. Am. Chem. Soc.*, 80(6): 1339.

13. Lu, W., Liu, S., Qin, X., Wang, L., Tian, J., Luo, Y., Asiri, A. M., Al-Youbi, A. O., and Sun, X., (2012). "High-yield, large scale production of few-layer graphene flakes within seconds: using chlorosulfonic acid and H₂O₂ as exfoliating agents", *J.Mater.Chem.*, 22: 8775-8777.
14. Dreyer, D. R., Park, S., Bielawski C. W., Ruoff. R. S., (2010). "The chemistry of graphene oxide", *Chem. Soc. Rev.*, 39: 228-240.
15. Xing, Z., Chu, Q., Ren, X., Tian, J., Asiri, A. M., Alamry, K. A., Al-Youbi, A. O., Sun, X., (2013) "Biomolecule – assisted synthesis of nickel sulfides/reduced graphene oxide nanocomposites as electrode materials for supercapacitors", *Electrochem. Commun.*, 32: 9-13.
16. Dimiev, A. M., Tour. J. M., (2014). "Mechanism of Graphene Oxide Formation", *ACS Nano.*, 8(3): 3060-3068.
17. Ganhua Lu, Shun Mao, Sungjin Park, Rodney S. Ruoff, Junhong Chen., (2009). "Facile, Noncovalent Decoration of Graphene Oxide Sheets with Nanocrystals", *Nano Res*, 2: 192-200.
18. Dresselhaus, M. S., Jorio, A., Saito. R., (2010). "Characterizing Graphene, Graphite, and Carbon Nanotubes by Raman Spectroscopy", *Annu. Rev. Condens. Matter Phys.*, 1: 89.
19. Ferrari, A. C., Basko. D M., (2013). "Raman spectroscopy as a versatile tool for studying the properties of graphene", *Nat. Nanotech.* 8: 235-246.
20. Cancado, L. G., Jorio, A., Martins Ferreira, E. H., Stavale, F., Achete, C. A., Capaz, R. B., Moutinho, M. V. O., Lombardo, A., Kulmala, T. S., Ferrari, A. C., (2011). "Quantifying defects in graphene via Raman spectroscopy at different excitation energies", *Nano Lett.*, 11: 3190-3196.
21. Kaniyoor, A., Ramaprabhu. S., (2012). "A Raman spectroscopic investigation of graphite oxide derived graphene", *AIP Advances* 2., 032183.
22. Eigler, S., Dotzer, Ch., Hirsch. A., (2012). "Visualization of defect densities in reduced graphene oxide", *Carbon.*, 50:3666.
23. Shang, J. Z., Ma, L., Li, JW., Ai, W., Yu, T., Gurzadyan, G. G., (2012). "The Origin of Fluorescence from Graphene Oxide", *Sci. Rep.*, 2: 792.